Eddy Current Damper for the Labshare Remote Laboratory Shake Table Rig

Peter A. Watterson, LaReine A. Yeoh, Carlo Giampietro, Christopher M. Chapman & Luke E. Houghton,
Faculty of Engineering and Information Technology
University of Technology, Sydney
Broadway NSW Australia
Peter.Watterson@uts.ed.au

***Abstract*—The design and performance of an eddy current damper for the *Labshare* remotely operated "Shake Table" multi-storey building vibration rig is described. The damper comprises stationary E-cores on either side of a copper plate attached to each storey. An approximate formula for the damper retarding force F is derived, of the form $F = -kuI^2$ for plate velocity u and E-core current I, and a criterion for its validity is established in terms of the magnetic Reynolds number. A close fit to measurements of the force using a load cell is obtained for k = 0.401 N/(ms^{-1}A^2). This was about 12% lower than the force determined by three-dimensional (3D) finite element analysis (FEA) using ANSYS 12.1, but the error can be attributed to manufacturing imperfections. Students can use the force formula in their investigation of closed-loop control of the Shake Table vibration. More generally, a formula for the force constant k can be used for the approximate design of any similar E-core damper.**

Keywords-eddy current damping; finite element analysis; remote access laboratory.

I. INTRODUCTION

A consortium of Australian universities have formed *Labshare Australia* to develop a network of laboratories with experimental rigs that students can operate remotely via the internet [1]. The "Shake Table" rig models the vibration of a multi-storey building in an earthquake [2]. Six units have been built and commissioned at the University of Technology, Sydney (UTS), 5 with 2 stories or 2 Degrees of Freedom, as shown in Fig. 1, and 1 with 3 Degrees of Freedom. The building motion is generated by a rotary motor with a scotch yoke producing a small sinusoidal linear oscillation of the building's ground level. Students calculate the resonant modes of vibration, select the frequency, and witness the motion on live video and LabView charts of the level displacements, measured by non-contact magnetoresistive sensors. The vibration suppression of a beam using eddy currents induced by permanent magnets has been proposed and analysed in [3]. Here an electromagnet damper is installed on each building level to enable separate control of the damping force for each level. This paper describes the design of the eddy current damper using magnetic circuit analysis, and compares the measured performance of the damper with both the design calculations and accurate 3D finite element analysis (FEA) results.

The electromagnet damper provides a variable non-contact braking force by inducing eddy currents in a copper plate attached to the building level. The damper configuration chosen was that of dual E-cores, one positioned on either side of the plate, as shown in Figs. 2 and 3. The two coil currents are in series and in the same direction in order that the flux primarily crosses from one E-core to the other through the plate. More precisely, the magnetic field topology created is that of two flux loops, one on each end of the E-core, with each loop crossing the plate twice. The E-cores were very cheap and easily wound on commercial bobbins. The cores would have been more easily held, countering the attractive force between them, if cores with corner holes had been available, but gluing the laminations and clamping the cores between perspex towers proved adequate. An alternative configuration, avoiding the difficulty of having to counter the attraction force across the gap, would be to have the plate moving in the gap of a C-core, as used in [4]. However, the dual E-core topology has greater force per mass.

The dual E-core topology was also recently analysed and tested in [5] but throughout that paper it was claimed that the coil currents should be in opposite directions and would produce much higher force then than for currents in the same directions (see in particular the current direction inset diagram of their Fig. 2 and their boundary conditions A-3). Their 2D Fourier analysis followed [6] in representing the currents as thin sheets on the core surfaces facing the gap, but [6] assumed equal current densities of the same sign on the two sheets. It appears that both the analytic solution and the measured forces in [5] were in fact for coil currents in the same directions.

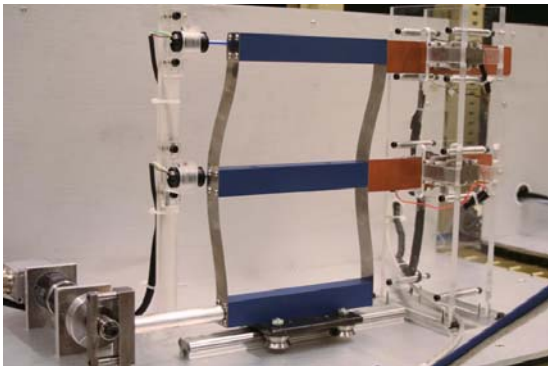

Figure 1. Shake Table rig with 2 Degrees of Freedom oscillating at its second resonance, dampers housed in the perspex tower on the right.

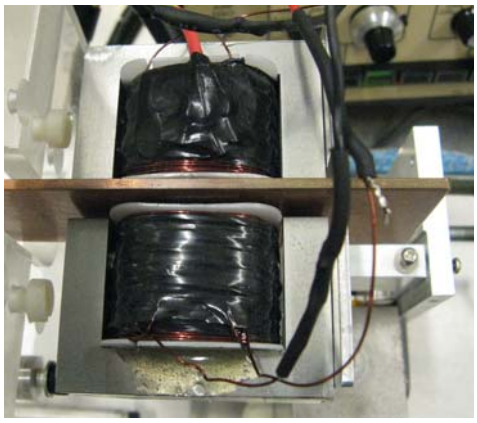

Figure 2. Photo of the damper during force testing, for which the E-cores were temporarily attached to a plate screwed to a load cell.

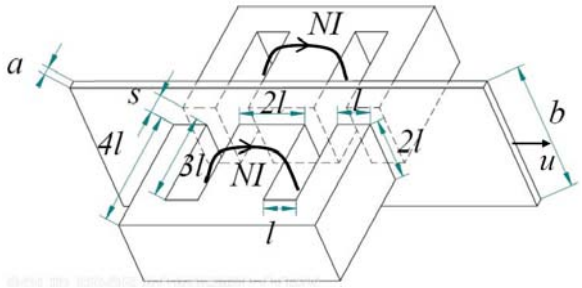

Figure 3. Dual E-core damper layout showing coil current directions and parameters. In our damper, l = 9.5 x 10^{-3} m, s = 6.3 x 10^{-3} m, a = 2.55 x 10^{-3} m and b = 40.5 x 10^{-3} m.

Here, an approximate analytic formula is derived for the dual E-core damper force, and accurate 3D finite element analysis (FEA) is reported and shown to agree well with measurements. An FEA solution for the case of coil currents in opposite directions shows it to have much lower force.

II. Magnetic Circuit Analysis

A theoretical understanding and rough estimate of the eddy currents and retarding force is now established using magnetic circuit analysis. The geometric variables of the E-core damper are shown in Fig. 3, including plate thickness a, plate width b, and E-core separation s. The clearance gap g on each side of the plate is related by

$$s = a + 2g. \tag{1}$$

The E-core dimensions are all multiples of a base length l, equaling the slot opening and the outer limb width; the centre limb has a square section of length $2l$, and the slot depth is $3l$. A copper plate was used with resistivity measured (by the voltage across an internal interval of a thin strip carrying current) as 3% higher than that of pure copper η = 1.72 x 10^{-8} Ωm, but the difference could be attributed to measurement imprecision (mainly in the strip width) and so pure copper resistivity is assumed. In order to keep the restriction of the eddy current loops low, the strip width b was chosen to keep the distance from the core to the plate edge slightly larger than l, i.e. b slightly larger than $4l$, which matches the width of the coil.

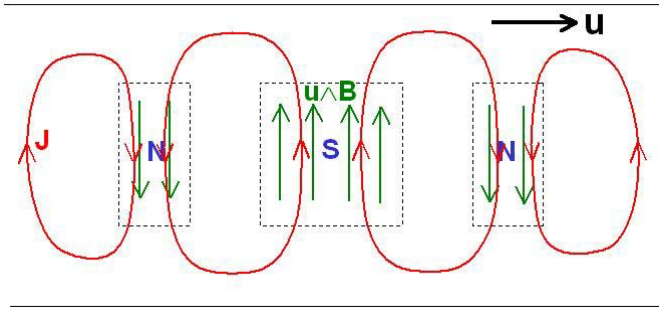

Figure 4. Sketch of the E-core's imposed magnetic flux density pattern (North and South poles bounded by dashed lines) and induced eddy currents $\boldsymbol{J}$ in the plate.

The analysis is built on the constitutive relation in the plate

$$\boldsymbol{E} + \boldsymbol{u} \wedge \boldsymbol{B} = \eta \boldsymbol{J} \tag{2}$$

where $\boldsymbol{E}$ is the electric field (in the stationary core reference frame), $\boldsymbol{B}$ the magnetic flux density, η the resistivity, $\boldsymbol{J}$ the current density, and $\boldsymbol{u}$ the plate velocity, approximated as $u(t)\hat{\mathbf{x}}$, see e.g. [7]. From magnetic circuit analysis, the typical static B across the plate produced by the coil currents can be stated as

$$B \approx f_1 \frac{\mu_0 NI}{s} \quad , \tag{3}$$

where f_1 is a factor introduced to account for fringing, N is the number of turns in each coil (in our system N = 380 was found to give convenient driving voltage), and I is the current in each coil. Because fringing makes the flux density lower in the plate than in the air gap, an f_1 less than 1 is anticipated, though in what follows we neglect the flux outside the core pole projections, which would increase the required value of f_1.

To proceed, we assume that the eddy currents produce magnetic flux densities much smaller than the static E-core field, examining later what conditions make this is valid. We will also adopt the quasistatic approximation of neglecting the time variation in $\boldsymbol{B}$ caused by the sinusoidal time variation in $u(t)$. Certainly for the maximum vibration frequencies to be used in the device here, around f = 10 Hz, the standard skin depth in copper is 21 mm, much larger than the copper plate thickness of a = 2.55 mm [8]. However, even for constant velocity u, there is an effective oscillation timescale being the time it takes for a point in the plate to move under a core pole, namely l/u (taking the shorter core side limb, being the shorter time). Providing the low eddy current assumption is valid, the quasistatic approximation can be adopted in the case when the vibration period is much longer than the l/u timescale, which is when the amplitude of the vibration is much larger than l.

With the assumption of a quasistatic u and hence quasistatic $\boldsymbol{B}$, by Faraday's law, the electric field $\boldsymbol{E}$ in the plate can be approximated as having zero curl and can be written

$$\boldsymbol{E} = -\nabla\phi \, , \tag{4}$$

for electric potential ϕ. As sketched in Fig. 4, the $\boldsymbol{u} \wedge \boldsymbol{B}$ term drives eddy currents $\boldsymbol{J}$ over the E-core poles. The resistance

over the broad current paths connecting the poles reduces the $\boldsymbol{J}$ over the poles by some geometric factor $f_2 < 1$ to

$$J \approx f_2 \frac{uB}{\eta} \quad , \tag{5}$$

with $\boldsymbol{E}$ opposing $\boldsymbol{J}$ over the poles but driving it outside the poles. The geometric factor f_2 corresponds to the dimensionless drag coefficient G introduced by [4], who established some analytic values for it in the case of a single square pole (whereas our case is of a chain of 3 poles). If the field generated by the eddy currents is much less than the static field of the cores, then the retarding force can be calculated by integrating $\boldsymbol{J} \wedge \boldsymbol{B}$ under the core poles (neglecting fringing) as

$$F \approx -(aA)JB \quad , \tag{6}$$

where A is the total E-core area facing the plate on one side, i.e. $A = 8l^2$. Substituting (3) and (5) leads to

$$F \approx -kuI^2 , \tag{7}$$

where

$$k = f\left(\frac{a}{s}\right)\frac{A\mu_0{}^2N^2}{\eta s} \quad , \tag{8}$$

introducing a combined geometric factor

$$f = f_1{}^2 f_2 . \tag{9}$$

Certain design guidelines can be gained from (8) assuming f can be taken as constant. For fixed ratio of plate thickness to separation, i.e. fixed a/s, the force constant k increases as the separation s decreases. However, this is only valid up until saturation in the core and any further reduction in the separation would reduce the force. Hence design to just on saturation is optimum. However, in our case, large clearance gaps g were required and the steel was well below saturation.

For a given fixed clearance gap g, it is straightforward to analytically determine, by substituting (1) into (8) and differentiating with respect to a, that the plate thickness a which optimizes the force constant k is

$$a_{opt} = 2g , \tag{10}$$

equivalently the plate should occupy half the separation.

Although uncertainty in the factor f makes k imprecise, the above theory was sufficient for E-core sizing for the Shake Table as the required force was not precisely known. The value $f = 0.7$ was assumed and a suitable commercial E-core size was chosen based on an acceptable temperature rise. The clearance gap had to be made larger than anticipated due to lateral oscillations of the building model. For the final dimensions reported above, the calculated force constant was k = 0.431 N/(ms^{-1}A^2).

To assess when the assumption that the magnetic field from the eddy current will be less than the static field of the core, the ratio of the driven eddy currents in the plate can be compared to the coil current. This is a conservative indicator as the field from the twin eddy current loops is reduced by the fact that its field does not align as well with the iron teeth as the field of the coil currents. The ratio of total eddy current I_e under the central E-core limb to the sum of the coil currents $I_c = 2NI$ is readily shown by integrating (5) through the plate under the central limb to be

$$\frac{I_e}{I_c} = f_1 f_2 \left(\frac{a}{s}\right) R_m , \tag{11}$$

where

$$R_m = \frac{\mu l u}{\eta} \tag{12}$$

is called the magnetic Reynolds number [9], with permeability $\mu = \mu_0$ for copper. The geometric ratio $a/s < 1$ is the fraction of the separation between the cores occupied by the plate. In our case, a/s = 0.40 and for a typical peak velocity u = 0.25 ms^{-1}, R_m = 0.17. Thus $\frac{I_e}{I_c} \ll 1$ and the assumption of a small eddy current magnetic field is valid. When this is not case, the total field will appear to be dragged "downstream" by the plate motion.

The significance of the magnetic Reynolds number R_m is commonly reported, though some others have defined it as the ratio of the eddy current flux density to the imposed flux density [10], instead of noting the dependence of that ratio on the expression (12), which is the magnetic equivalent of the dimensionless fluid dynamics Reynolds number. ANSYS provide for evaluation and plotting of the magnetic Reynolds number based on each element's dimension (in place of the macroscopic length scale l of our E-core in (12)), and warn that solutions become inaccurate when this number approaches 1 [11, Section 2.3.1.9].

III. Finite Element Analysis

FEA of the E-core damper has been undertaken for the quasistatic approximation of the plate velocity taken as constant using ANSYS 12.1 [11]. ANSYS can solve for the eddy currents in a moving solid conductor under conditions which are valid here, namely: linear B-H curves, so below saturation steel (relative permeability μ_r = 1000 was assumed here); and "the moving body presents itself as a homogeneous moving body for which the moving "material" undergoes no spatial change" [11, Sections 2.3.1.8 and 9.4.1.3]. This is valid in our case providing the ends of the moving plate are sufficiently distant from the core, and are assumed beyond the solution domain. The static solution with moving conductor is performed using their "harmonic analysis" capability with a very low frequency (we used 0.001 Hz), though the velocity is actually constant. Results here are for the edge-based SOLID117 element, found to be far superior to the vertex-based SOLID97 element.

Solutions were obtained over one quarter of the damper using appropriate symmetry boundary constraints across the plate and core mid-planes. The force was inferred by dividing the integrated eddy current ohmic dissipation in the plate by the

velocity. The mesh was refined until the solution had converged to within a few percent.

The FEA solution for the damper built with velocity u = 0.25 ms^{-1} is documented in Figs. 5 to 9. The velocity is in the positive x direction, and the z direction is normal to the plate. The $\boldsymbol{B}$ vector plot of Fig. 6 shows considerable flux fringing, expected for this large core separation case. Consequently the peak B_z in the plate is twice as large under the centre limb compared to the side limb (see Fig. 7). The induced eddy current pattern, Fig. 8, is of the form anticipated in Fig. 4, with the outside current loops much smaller in amplitude than the central loops. The small magnetic field produced by the eddy currents causes a slight asymmetry in the fields; for instance, Fig. 9 shows that the normal flux density in the plate mid plane is about 3% higher on the "downwind" side, i.e. in the direction of the plate velocity.

From the calculated force, the inferred $k = 0.456$ N/($ms^{-1}A^2$) in (6) and $f = 0.742$ in (8).

As a check on linearity of the force with velocity, a solution was obtained with quadruple the velocity, u = 1 ms^{-1}, and the force was found to be just 2.0% below linear. From (11) and (12) with u = 1 ms^{-1}, it is evident that the product of magnetic Reynolds number R_m = 0.69 and factor a/s = 0.40 in combination was sufficiently low to keep the eddy current magnetic field small enough to maintain linearity of the force with velocity.

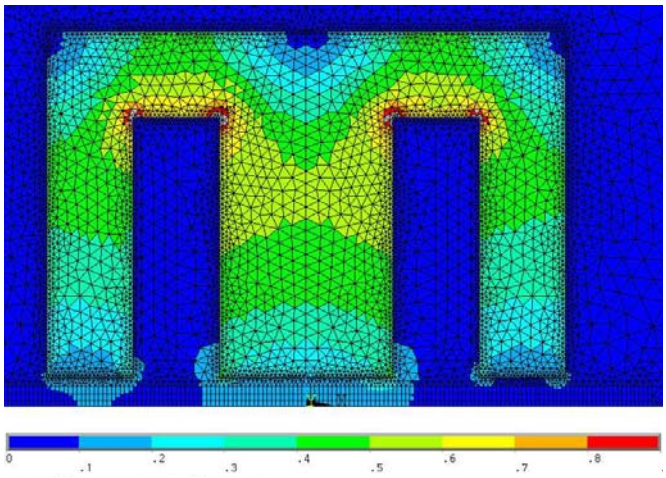

Figure 5. Magnetic flux density amplitude mid core, contours 0 to 0.9 T.

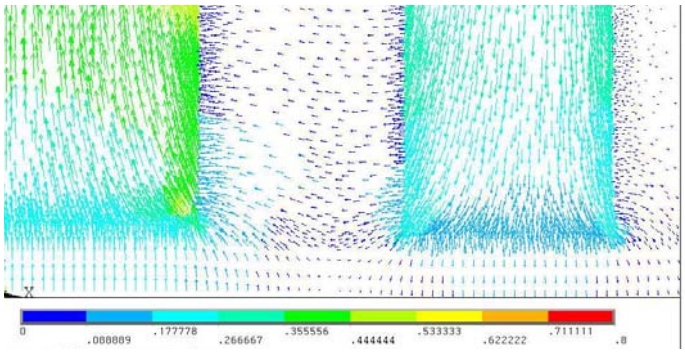

Figure 6. Magnetic vectors near the core tips at the core mid plane, showing flux fringing, amplitude contours from 0 to 0.8 T.

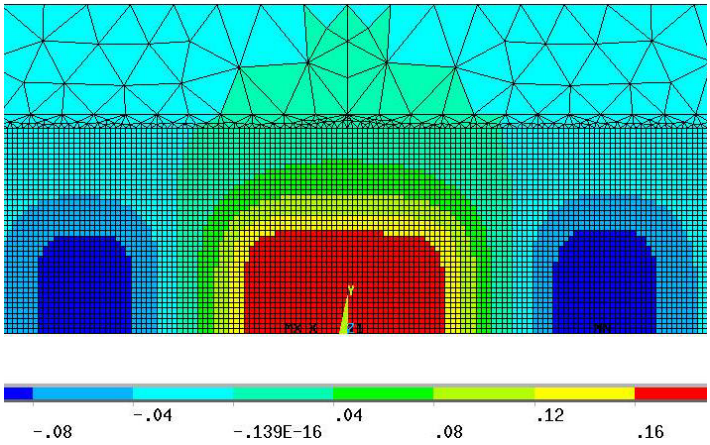

Figure 7. Normal component B_z mid plate, contours from -0.12 to 0.20 T.

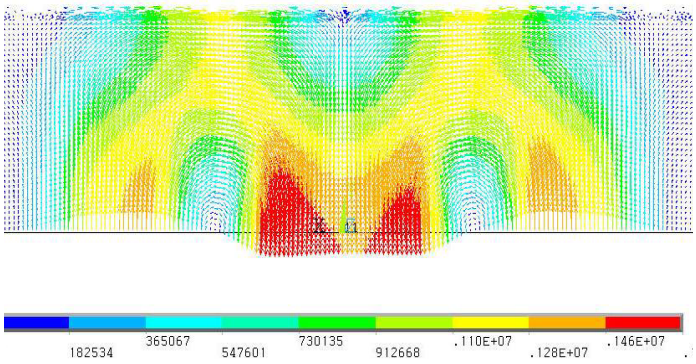

Figure 8. Eddy current vectors mid plate, amplitude contours from 0 to 1.64 x 10^6 Am^{-2}. Note that currents are very slightly larger "downwind" of the velocity, i.e. towards x > 0, which is to the left in this plot.

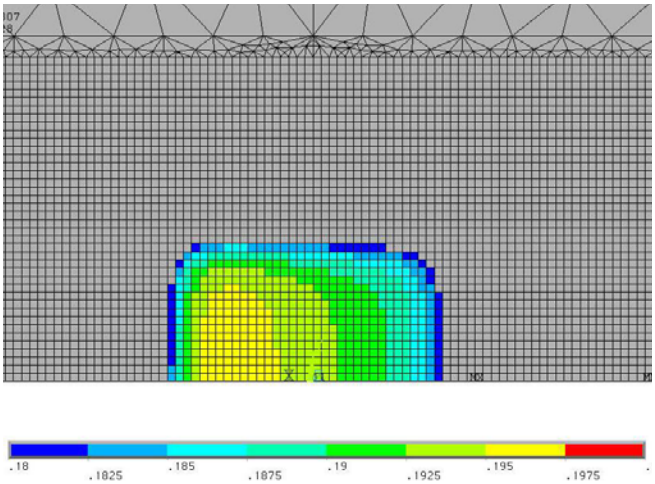

Figure 9. Close up of component B_z mid plate under the centre limb, contours from 0.18 to 0.20 T showing a slight asymmetry about $x = 0$.

In order to evaluate the range of variation of the geometric factor f in (8), FEA solutions were obtained for a 2 x 2 array of cases (the above solution being one of them). The cases had either a large or a small separation s compared to the core length parameter l, and one of two values of a/s, the fraction of the separation filled by the plate, each on either side of the optimum value 0.5 (as stated in (10)). The results given in

Table I show that f is nearly independent of a/s over the range 0.4 to 0.6 and f varies from around 0.57 for the small gap s/l = 0.133, to 0.75 for the large gap s/l = 0.663. These values are all for the assumed plate width b/l = 4.26 and f is also a weakly increasing function of b/l. Nevertheless, we can conclude that a useful approximate design rule would be to either use the average value f = 0.66 (close to our original estimate of 0.7) or, for more precision, to use the simple linear relation

$$f \approx 0.34\left(\frac{s}{l}\right)+0.52\,, \qquad (13)$$

checked over the range $0.1 < s/l < 0.7$.

As a quick test of the claim in [5] that the coil currents in the E-cores should be in opposite directions, the FEA solution was obtained by changing the mid plate boundary condition to magnetic flux parallel instead of perpendicular. Fig. 10 shows the calculated $\boldsymbol{B}$. The calculated force constant was k = 0.0016 N/(ms^{-1}A^2), only about 0.4% of the case where the coil currents are in the same directions, providing further confirmation that the authors seem mistaken in their claim [5].

IV. Experimental Measurements

Measurements of the force and velocity were obtained for the E-core damper with the copper plate of a Shake Table level undergoing free vibration. The force was measured on a pair of E-cores taken from their support tower and temporarily glued to a plate attached to a single point load cell (Vishay Model 1004), rated to 6 N. The position was recorded using the system's non-contact magnetoresistive linear position transducer (Temposonics, made by MTS Systems Corporation, Cary USA) and data acquisition was by LabView at 500 Hz sampling frequency. The coil current was supplied by the system's current source amplifier, which maintains the current constant as coil temperature varies. Data was taken for 4 different currents over the range of interest.

TABLE I. Geometric scaling factor f of (8) inferred by FEA (for relative plate thickness b/l = 4.26)

Factor f		**Core separation relative to fundamental length, s/l**	
		0.133	***0.663***
Fraction of gap occupied by plate, a/s	***0.405***	0.569	0.742
	0.595	0.570	0.753

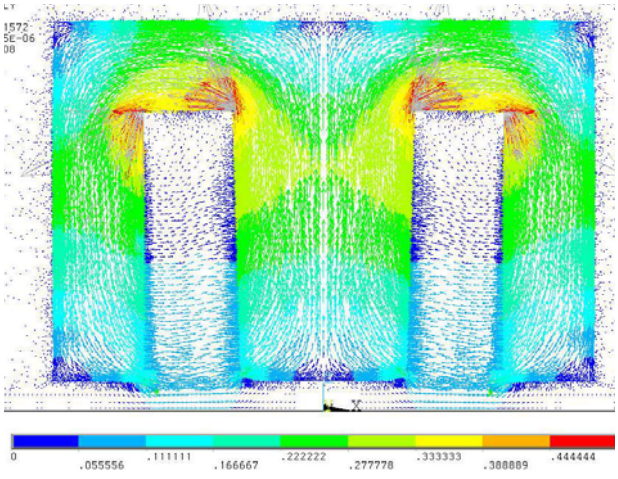

Figure 10. $\boldsymbol{B}$ vectors in the core mid plane for the case of opposite directed coil currents with zero perpendicular $\boldsymbol{B}$ at the plate midplane.

Smoothing was needed to infer the velocity from the position signal and the method chosen was the Lanczos differentiator [12]

$$\left(\frac{dx}{dt}\right)_0 = \frac{x_1 - x_{-1} + 2(x_2 - x_{-2}) + 3(x_3 - x_{-3})}{28(\Delta t)}\,, \qquad (14)$$

where Δt is the timestep, which evaluates the gradient of the quadratic fit to a sliding window of 7 data points.

A window in the decay of the vibration for current I = 2.00 A is shown in Fig. 11. Fig. 12 plots force versus velocity, showing that the dependence is close to linear. The line of best fit is calculated (using standard least squares fitting). This procedure was repeated for the recordings from the other current values and the inferred force/velocity gradients are plotted in Fig. 13. The best fit to the squared law (7) was obtained by minimizing the squared errors yielding k = 0.401 N/(ms^{-1}A^2), corresponding to f = 0.653 in (8). This is

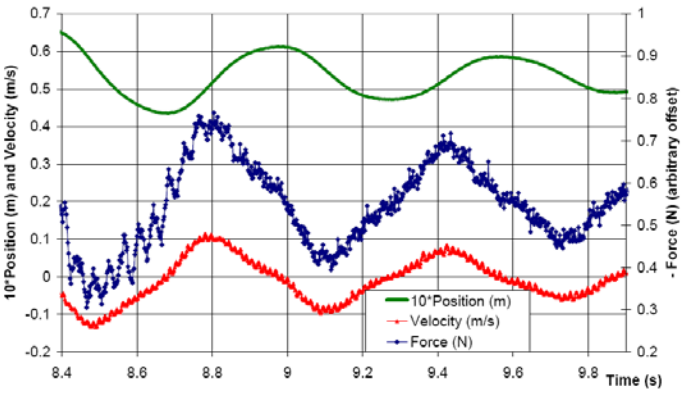

Figure 11. Variation with time of position (multiplied by 10) and velocity (both against the left axis) and (negative) force (right axis) for I = 2.00 A.

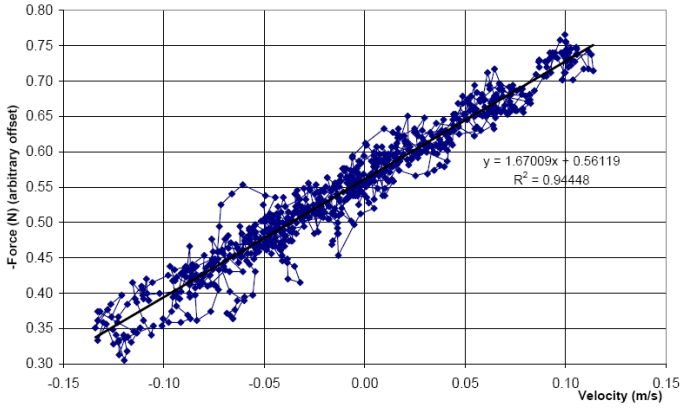

Figure 12. Measured –force v. velocity over 2 cycles for I = 2.00 A, with least squares line of best fit.

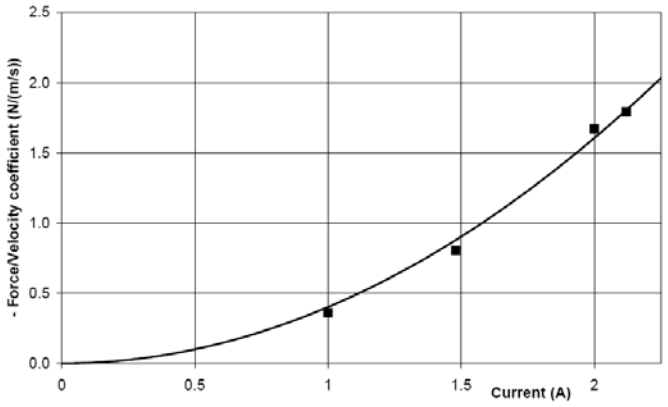

Figure 13. Force/velocity gradients v. current with best fit quadratic 0.401 I^2.

12% lower than the k (and f) inferred from the FEA, 0.456 N/(ms^{-1}A^2). This difference may be attributed either or both to a slight increase in the resistivity of the copper plate above pure copper (measurements suggested this was by around 3%) and to manufacturing variations in the damper – in particular, the separation s was 6.3 x 10^{-3} m over most of the cores' transverse width but flared out at one end to about 7 x 10^{-3} m due to imperfect gluing of the laminations.

V. Conclusions

The analytical design, FEA and testing of a dual E-core eddy current damper has been reported. Magnetic circuit analysis led to the approximate design formula (7) - (8) with geometric factor f. The formula should be valid providing the iron remains below saturation and the induced eddy currents are smaller than the applied currents, which may be assessed by (11), involving the magnetic Reynolds number (12) and geometric factors f_1 and f_2 which may be taken as 1 and 0.7 respectively. For given clearance gap g, the optimum plate thickness a is given by (10).

FEA has been used to confirm the magnetic circuit analysis and establish suitable approximate values for the force factor f by which other E-core dampers could be designed. For standard E-cores whose dimensions can be defined in terms of their slot opening l, there are 3 dimensional parameters defining the dual E-core damper geometry. Here one of these, the relative conducting plate width b/l, was fixed at around 4 (4.26 to be precise). The factor f would be slightly increased for wider plates and reduced for smaller plates. Factor f was found to have virtually no dependence on the plate thickness relative to the core separation a/s in the vicinity of its optimum value 0.5, and to have a weak dependence on the relative separation s/l, which could be modeled by the linear expression (13). But to within ±15% over the range $0.1 < s/l < 0.7$, one could simply take f as the constant $f = 0.66$.

Measurements on a damper in use on the Shake Table rig confirmed the force varied as uI^2 and yielded $f = 0.653$, just 12% lower than the FEA calculated factor for its dimensions, $f = 0.742$. This represents very good agreement between theory and experiment, allowing for the manufacturing variation in the damper, which had slightly increased separation over some of its width.

For practical application of this study to the Labshare Shake Table, all that needs to be known is that the damping force behaves according to the simple formula (7) and the constant can be taken as $k = 0.40$ N/(ms^{-1}A^2) assuming core separation $s = 6.3$ x 10^{-3} m. There is inevitably some variation between dampers in their core separation, and the force will vary inversely with s^2, as per (8).

In the Shake Table rig, position data acquisition and control are implemented using a LabJack UE9. For completeness it is noted that the proportionality between the LabJack control signal output voltage V and the driven coil current (after the current source amplifier) is $I \approx (0.548$ A/V$)\ V$, with I limited to about $I = 2.04$ A to minimise overheating.

Armed with the above model for the damper force, students can design optimal strategies for building vibration control. Others wishing to design dual E-core dampers for other applications can use the simple formulae established.

Acknowledgment

Jianchun Li, Dikai Liu, Lothar Weber, Michel De La Villefromoy, Michael Diponio, Polycarpos Papatheodotou, Richard Turnell, Kurt Friday, Richard Moore and Ron Smith are thanked for their contributions to the Shake Table development.

References

[1] Labshare Australia homepage, www.labshare.edu.au on 2/6/10.

[2] L. Yeoh, "Remote Shaker Table Laboratory User Guide Version 1.0", Remote Laboratories, Faculty of Engineering and IT, University of Technology, Sydney, 2009.

[3] J.-S. Baea, M.K. Kwakb and D.J. Inman, "Vibration suppression of a cantilever beam using eddy current damper", J. of Sound and Vibration vol. 284, pp. 805–824, 2005.

[4] M.R. Weinberger, "Drag Force on an Eddy Current Damper", IEEE Transactions on Aerospace and Electronic Systems, vol. AES-13, No. 2, pp. 197-200, March 1977.

[5] R. K. Srivastava and S. Kumar, "An Alternative Approach for Calculation of Braking Force of an Eddy-Current Brake," IEEE Transactions on Magnetics, vol. 45 no. 1, pp. 150-154, January 2009.

[6] S. Yamamura, H. Ito and Y. Ishulawa, "Theories of the Linear, Induction Motor and Compensated Linear Induction Motor," IEEE Transactions on Power Apparatus and Systems, vol. PAS-91, no.4, pp.1700-1710, July 1972.

[7] W. R. Smythe, Static and Dynamic Electricity, McGraw-Hill Book Co., New York, NY, 1950.

[8] P. Lorrain and D. Corson, Electromagnetic Fields and Waves, 2nd Ed., W.H. Freeman and Co, San Francisco, p.478.

[9] H.K. Moffatt, Magnetic Field Generation in Electrically Conducting Fluids, p. 47, Cambridge University Press, Cambridge UK, 1978.

[10] K. Lee and K. Park, "Eddy Currents Modeling with the Consideration of the Magnetic Reynolds Number", Proc. IEEE International Symposium on Industrial Electronics, ISIE 2001, vol.1, pp.678-683, 2001.

[11] ANSYS Release 12.1 "Mechanical APDL" software and Low Frequency Electromagnetic Analysis Guide, ANSYS Inc., Canonsburg, PA, USA, November 2009.

[12] C. Lanczos, Applied Analysis, p.321, Dover, Mineola N.Y. USA, 1988.